COHERENT ELECTRON COOLING: STATUS OF SINGLE-PASS SIMULATIONS*

B.T. Schwartz†, G.I. Bell, D.L. Bruhwiler‡, I. Pogorelov, S.D. Webb
Tech-X Corp., Boulder, CO 80303, USA
V.N. Litvinenko, Y. Hao, G. Wang, BNL, Upton, NY 11973, USA
S. Reiche, Paul Scherrer Institut, Villigen PSI, 5232, Switzerland

Abstract

Advances in nuclear physics depend on experiments that employ hadron accelerators with dramatically increased luminosity. Stochastic cooling is currently used to increase hadron beam luminosity, but this approach faces serious difficulties at the high intensities and high energies proposed for high-energy election-ion colliders. The novel concept of coherent electron cooling (CeC) promises to cool hadron beams at a much faster rate. Simulations of a single pass through a CeC system are key to its experimental demonstration. Here we validate the primary components of these simulations.

INTRODUCTION

Coherent electron cooling is a method for increasing hadron accelerator luminosity, which is required for advances in nuclear and particle physics [1]. Unlike standard electron cooling, which uses dynamical friction to cool ions [2], coherent electron cooling relies on anisotropic Debye shielding that imparts perturbations in charge density and velocity onto the electron beam [3].

These perturbations enable a free electron laser (FEL) to lase via self-amplified spontaneous emission (SASE). The lasing amplifies the electron density modulation and imparts on it a sinusoidal modulation with a period equal to the FEL wavelength $\lambda_{\rm FEL}$. This longitudinal space charge provides a coherent kick designed to reduce the bunch energy spread. [1, 4]. In the current proof-of-principle experimental design (CeC PoP) [5], the electrons are shifted to achieve correct phasing such that the slower ions are accelerated while the faster ions are decelerated, which results in cooling.

ION SHIELDING IN THE MODULATOR

In the modulator section of the CeC PoP experiment, gold ions copropagating with an electron beam perturb the electron density. Analytic results have been derived for the case of Debye shielding by an infinitely wide electron plasma with a Lorentzian velocity distribution [6]. Here we validate VSIM [7] δf Particle-in-Cell (PIC) simulations [8] for this case by comparing the results to these analytical predictions.

In these 3D simulations, an Au^{+79} ion with longitudinal velocity $v_z = 3.0 \times 10^5$ m/s is shielded by a plasma with density $n_e = 1.1 \times 10^{16}$ m^{-3} and $v_z^{\rm rms} = 3.0 \times 10^5$ m/s. Its transverse and longitudinal Debye lengths were $\lambda_{D\perp} = 385$ μm and $\lambda_{Dz} = 50.5$ μm, respectively. The grid spacings were 0.125 Debye lengths, with 600 macro-particles per cell. The high resolution and large numbers of particles required parallel simulations using thousands of processors.

Equilibrium Debye shielding around a single Au^{+79} ion produces an excess of ~ 79 electrons among $\sim 10^7$ physical electrons in the relevant domain. Since the simulation domain is finite, the simulation boundaries are set up to allow a thermal flux of electrons to leave and enter them. Electrons near the boundaries that had just recently entered the simulation domain have inaccurate positions and velocities, as they have only begun to experience the fields from the ion and other electrons.

Hence, only the central portion of the domain is shown in the Fig. 1, which show the agreement of VSIM simulations done with Lorentzian electron velocity distributions with theory. This validates the accuracy of the same simulations done with the physically realistic Maxwellian velocity distribution.

BUNCHING & ENERGY MODULATION

We coupled the output from the modulator simulations to GENESIS, a well-established FEL simulation code [9].

Table 1: Electron and Ion Beam Parameters, Beam Frame *

e-beam parameter	value
electrons per bunch N_e	4.7×10^9
peak current	80 A/γ_e
emittance, rms-normalized	5 mm-mrad
Twiss $\hat{\beta}$ (start,end)	4.5, 1.5 m †
number density (end) n_e	2.78×10^{16} m^{-3}
$\delta\gamma_e/\gamma_e$	0.001 (lab frame)
rms velocity $v_z^{\rm rms}$	3.00×10^5 m/s
$\lambda_{\rm Debye}$ (end) $\lambda_\perp, \lambda_z$	385, 50.5 μm
ion parameter	**value**
v_z (Au^{+79} ion)	3.00×10^5 m/s

* γ_0=43.66, both beams.
† "start" & "end" denote e-beam position in modulator.

* Work supported by the US DOE Office of Science, Office of Nuclear Physics, in part through the SciDAC project ComPASS and in part through the SBIR program, contracts DE-FC02-07ER41499 and DE-FG02-08ER85182. We used resources of NERSC, DOE contract No. DE-AC02-05CH11231.

† btschwartz@txcorp.com
‡ current affiliation: University of Colorado, Boulder

ISBN 978-3-95450-122-9

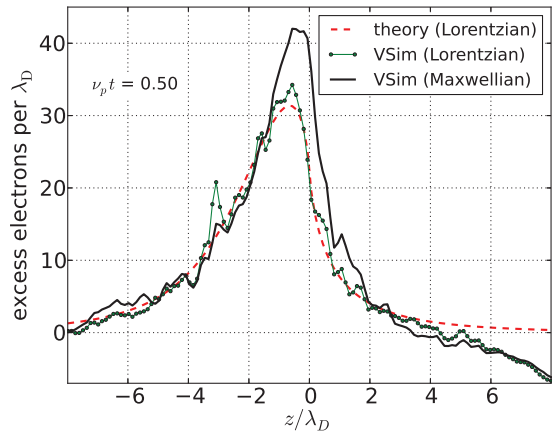

Figure 1: VSIM δf PIC computation of longitudinal on-axis electron density perturbation near a Au^{+79} ion with a non-zero longitudinal velocity in an anisotropic plasma.

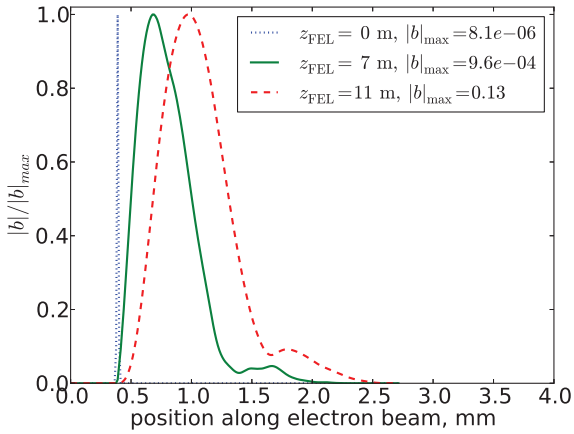

Figure 2: Normalized bunching magnitude, at λ_{FEL}, along the electron beam at different positions in the FEL. The bunching magnitude increased from $|b|_{min} = 8.1 \times 10^{-6}$ to $|b|_{max} = 0.13$.

This coupling involved computing the complex bunching parameter b at λ_{FEL}in a region containing N electrons, as described in Refs. [10] and [11]: $b = \frac{1}{N}\sum_{j=1}^{N} e^{i\theta_j}$, where $\theta_j = (k+k_w)z - ckt$ is the electron's ponderomotive phase and $k_w = 2\pi/\lambda_w$.

The bunching algorithm for particle distributions modeled using δf PIC differs slightly from the bunching expression above. With δf PIC, the $N = N_0 + N_1$, where N_0 denotes the equilibrium background electrons and N_1 represents the perturbation to this background. Since the background electrons do not contribute to bunching, the numerator is a sum only over N_1 electrons in the volume where bunching is computed. Since $N_1 \ll N_0$, the denominator need only include the N_0 electrons in the volume. Finally, since each macroparticle in the simulation represents N_{mp} electrons with a weight w_i, the bunching algorithm for δf PIC particles is

$$b = \frac{N_{mp}}{N_0}\sum_{j=1}^{N_1} w_j e^{i\theta_j}. \quad (1)$$

To validate Eq. 1, we performed ion shielding simulations in a regime where both standard PIC and δf PIC produced the same integrated one-dimensional charge density, $\rho_{1D}(z) = \int_x\int_y \rho(x,y,z)dxdy$. Since noise dominates standard PIC simulations for physical values of Z, we need used an ion with an artificially strong charge, $Z = 2200$. This is slightly less than the number of electrons in the plasma's Debye sphere, $N_e = 2900$.

For $\rho_{1D}^{\delta f}(z)$ to equal $\rho_{1D}^{PIC}(z)$, we increased the ion charge to Z=2500 in the δf PIC simulation. In both cases the plasma number density was $n_0 = 1.6 \times 10^{16}$ m^{-3} with a Debye length of $\lambda_D = 35.2$ μm.

We computed the bunching at λ_{FEL}= 12.5 μm in a λ_{FEL}-wide slice centered on the ion. The computed bunching magnitudes – for standard PIC and δf PIC – were within a factor of two of each other. The source of this difference may be that the δf PIC simulation is accurate when the number of electrons in a Debye sphere far exceeds the number of shielding electrons, which was not the case here. Future work will include a more rigorous PIC simulations using more particles, which will reduce noise such that shielding can be seen with smaller Z values.

Ion shielding imparts a modulation onto the electron energies in a similar way that it modulates their positions: $\gamma_{mod} = \frac{2}{N}\sum_{j=1}^{N}(\gamma_j - \gamma_0)w_j e^{i\theta_j}$.

To model the CeC PoP experiment, we computed the shielding around an ion in a finite electron beam ($r_{RMS} = 415$ μm), described in Table 1. The domain had transverse width of $10r_{rms}$. Each cell, measuring $\lambda_D/12$ on a side, contained 128 δf macroparticles.

The bunching magnitude in a λ_{FEL}-wide slice about the center of the ion was $|b| = 8.1 \times 10^{-6}$, with bunching factors decreasing by a factor of ten in the two adjacent slices. Similarly, the modulation of electron energy in the center slice was $\gamma_{mod} = 2.3 \times 10^{-6}$, with the γ modulation decreasing by more than a factor of 5 in adjacent slices.

FEL AMPLIFIER

Features of the GENESIS algorithm, combined with the short spatial scale of the non-trivial bunching coefficients b (compared to λ_{FEL}), prohibit directly loading particle phase space coordinates into it. The bunching information would be lost. Hence, we allowed GENESIS to create its own particles first, which represent the beam described in Table 1.

To distinguish the coherent bunching signal caused by the ion shielding from shot noise, we created particles in GENESIS using a quiet start. Per the GENESIS algorithm, they had linearly increasing ponderomotive phase θ_0 across each λ_{FEL}-wide slice of the electron beam (2^{15} macroparticles per slice). We added the bunching and γ modulations according to the expression used in the GENESIS source code [9]:

$$\theta_{bunched} = \theta_0 - 2|b|\sin(\theta_0 - \arg(b)) \quad (2a)$$

$$\gamma_{bunched} = \gamma_0 - \gamma_{mod}\sin(\theta_0 - \arg(\gamma_{mod})) \quad (2b)$$

Table 2: FEL Parameters

λ_w (helical)	4 cm	a_w	0.437
λ_{FEL}	12.5 μm	$\delta\nu$	420 GHz
$\tilde{r}_{rms}$, e-beam	415 μm	$\hat{\beta}$ (Twiss)	1.5 m

Since the electron beam is much longer than the region over which we computed the bunching, only particles in the leading few slices of the electron beam had non-zero bunching coefficients.

To validate this method, we used Eqs. 2a and 2b to add either bunching or energy modulation to a "quiet start" GENESIS particle distribution containing no initial bunching or energy modulation. We then computed the bunching and energy modulation values, and found them to agree with the initial values entered into Eqs. 2a and 2b.

Table 2 shows the FEL parameters for the CeC PoP experiment. The bunching introduced by the single ion increases as the electron beam travels through the FEL. In this coherent case, the peak bunching from ion shielding increased by two orders of magnitude, as shown in Fig. 2.

KICKER COMPARISON TO 1-D THEORY

In the kicker the peak magnitude of longitudinal electric field $E_z(z)$ varies in time. To validate that the field correctly evolves in our 3D VSIM simulations, we compare the charge density magnitude to a 1D theoretical prediction described in Ref. [4]. Figure 3 shows the results.

To minimize differences arising from the higher dimensionality of the simulations, we generated a quasi-1D simulation by setting the electrons' transverse velocities and transverse electric fields to zero. Accurate kicker simulations with input from the 7-m long FEL prescribed by the CeC PoP experiment requires resource-intensive computations with low-weight macroparticles to reduce noise. Hence, to validate our model, we extended the FEL length to 11 meters, which creates a stronger coherent signal.

The 1D theoretical prediction also depends on the FEL length. As described in Refs. [12] and [13], the 3D FEL gain length exceeds the theoretical 1D FEL gain length by a factor of $(1+\Lambda)$, where Λ is the length degradation factor. Hence, when comparing kicker field evolution of electrons exiting the $L_{\mathrm{FEL}} = 11.0$ m FEL modeled above, we scaled the FEL length by $(1 + \Lambda)$, which yielded an effective 1D FEL length of $L_{\mathrm{eff}}^{\mathrm{1D}} = L_{\mathrm{FEL}}/(1 + \Lambda) = 8.1$ m.

The agreement between theory and quasi-1D kicker simulations shown in Fig. 3 validates, at least qualitatively, the evolution of the longitudinal fields in the kicker. The differences between the theoretical and numerical predictions arise from to factors. First, our simulations are not truly 1D. Second, Ref. [13] notes that the fitting formula for computing Λ typically yields agreement with numerical FEL solutions to within 10%. We plan to do a true 1D simulation for improved validation.

CONCLUSIONS

Modeling a single pass of an ion through a coherent electron cooling system includes accurate simulations of a coherent signal imparted onto an electron beam before and after its amplification by a free-electron laser. This paper demonstrates how a freely available FEL simulation code and a δf PIC software package compatible with high-performance computers can achieve this. Future work includes larger simulations to improve accuracy, a true 1D kicker simulation to compare with theory, computing the cooling rate in a CeC system, and comparing this with cooling rates for a stochastic cooling system.

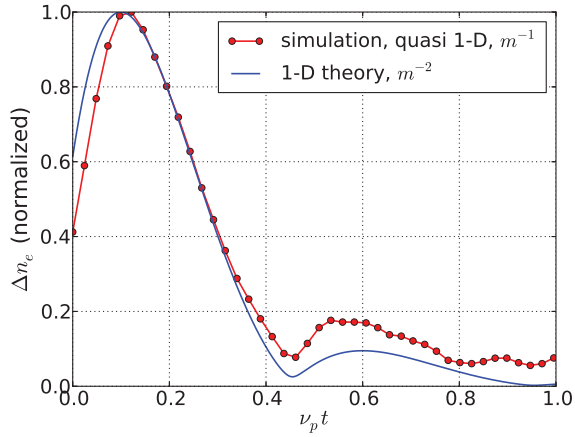

Figure 3: Peak magnitude of electron bunch charge density modulation as a function of its propagation time in the kicker.

ACKNOWLEDGMENT

The authors thank Gregg Penn at LBNL for guidance on computing energy modulation.

REFERENCES

[1] V.N. Litvinenko and Y.S. Derbenev. Phys. Rev. Lett, 102(11):114801, 2009.

[2] G. Bell, D. Bruhwiler, et al. J. Comput. Phys., 227(19):8714–8735, 2008.

[3] B.T. Schwartz, D.L. Bruhwiler, et al. Simulations of a Single-Pass Through a Coherent Electron Cooler for 40 GeV/n Au^{+79}. PAC'11, New York, MOP074, p. 244 (2011).

[4] G. Wang and M. Blaskiewicz, Progress of analytical modeling of coherent electron cooling. IPAC'10, Kyoto, MOPD077, p. 873 (2010).

[5] I. Pinayev et al. Status of proof-of-principle experiment for coherent electron cooling. IPAC'12, New Orleans, MOPPD016, p. 400 (2012).

[6] G. Wang and M. Blaskiewicz. Phys. Rev. E, 78:026413, 2008.

[7] VSim 6.0. Tech-X Corporation, Boulder, CO, USA.

[8] N. Xiang, J.R. Cary, et al. Phys. Plasmas, 13:062111, 2006.

[9] S. Reiche., *GENESIS 1.3*, 2004. `http://genesis.web.psi.ch`

[10] M.R. Jalal and F. Aghamir. Opt. Commun., 281(14):3771 – 3775, 2008.

[11] B. McNeil and G. Robb, *J. Phys. D*, 31(4):371, 1998.

[12] M. Xie. Nuclear Instruments and Methods in Physics Research A, 445:59–66, May 2000.

[13] Z. Huang and K.-J. Kim. Phys. Rev. ST Accel. Beams 10(3):034801, Mar 2007.

ISBN 978-3-95450-122-9